Universiteit Leiden
The Netherlands

Nuclear magnetic resonance force microscopy at millikelvin temperatures

Haan, A.M.J. den

Citation
Haan, A. M. J. den. (2016, March 9). *Nuclear magnetic resonance force microscopy at millikelvin temperatures*. *Casimir PhD Series*. Retrieved from https://hdl.handle.net/1887/38444

Version:	Not Applicable (or Unknown)
License:	Licence agreement concerning inclusion of doctoral thesis in the Institutional Repository of the University of Leiden
Downloaded from:	https://hdl.handle.net/1887/38444

Note: To cite this publication please use the final published version (if applicable).

Cover Page

Universiteit Leiden

Leiden University Repository

The handle http://hdl.handle.net/1887/38444 holds various files of this Leiden University dissertation

Author: Haan, Arthur den
Title: Nuclear magnetic resonance force microscopy at millikelvin temperatures
Issue Date: 2016-03-09

Chapter 7

Nuclear magnetic resonance force microscopy at millikelvin temperatures

This chapter is in preperation to be published with the following authors: J. J. T. Wagenaar*, A. M. J. den Haan*, J. M. de Voogd, K. M. Bastiaans, T. de Jong, D. J. Thoen, A. Endo, T. M. Klapwijk and T.H. Oosterkamp

*These authors have contributed equally

We report nuclear magnetic resonance force microscopy experiments down to temperatures of 42 mK, in which we measure nuclear spin relaxation times. We measured the Korringa relation between the nuclear relaxation time and temperature for a 300 nm thick copper sample. Performing local nuclear magnetic resonance experiments at such low temperatures enables an improvement in the microscope's sensitivity and opens up possibilities for future investigations of condensed matter systems at very low temperatures.

7.1 Introduction

During the last decade, a lot of progress has been made in understanding novel quantum materials and unresolved problems in high-Tc superconductors. Nuclear Magnetic Resonance has helped to study local magnetic fields and their inhomogeneities. A tool that could provide such information *on a local scale* would be very useful. State of the art Magnetic Resonance Force Microscopy (MRFM) has demonstrated a resolution smaller than 10 nm, by detecting proton spins in a virus particle [2]. MRFM has also shown to be able to measure relaxation times down to 4.8 K of nuclear spins in GaAs [106]. We demonstrate that MRFM can also be used to study the temperature

dependence of the relaxation time T_1 in copper, the so-called 'Korringa relation[1]', at low temperatures between 42 and 240 mK. We believe this opens up the possibility to use nanoscale NMR investigations of various materials, where electronic properties are inhomogeneous, such as in Topological Insulators in which bulk conductivity and surface conductivity can vary by orders of magnitude.

In most MRFM apparatus, the use of a laser in the readout of the motion of the cantilever, combined with RF currents that are applied using a copper or gold wire [30], prevent experiments at temperatures below 300 mK. We make use of a superconducting readout of the motion, combined with a superconducting RF-wire. We show that with this, we can reach local temperatures down to 42 mK, currently limited only by the performance of our dilution refrigerator. The local temperatures during magnetic resonance experiments are verified by measuring the Korringa law $T_1T = \kappa$ of a copper sample, with T_1 the relaxation time of the copper nuclei and T the (electron) temperature. κ is the Korringa constant, which is expected to be 1.2 sK [84, p. 225].

7.2 Experimental setup

The experimental setup is described in chapter 2 and closely resembles the setup described in chapter 6. A summary, with the relevant details of the experimental setup, is written below.

The cantilever's natural resonance frequency is 3.0 kHz with a mechanical quality factor $Q = 3 \cdot 10^4$, when far away from the surface. The sample under study can be approached coarsely in a range of 1 mm in x,y and z while reading out the position using three capacitive sensors. The sample holder is placed on a finestage which is used to control the z-position in a range of 2.3 μm. The fabrication of the sample is described in detail in section 2.4.

7.3 Methods

We positioned the cantilever above the copper, sufficiently close to the pick-up coil for a good coupling and close to the RF wire (as indicated by a small black dot in figure 7.1). Using the position of the center of the pick-up coil, which is found by maximizing the coupling of the magnetic particle with the pick-up coil, we determined the position to be 5 ± 1 μm from the pick-up coil and 7 ± 1 μm from the center of the RF wire. While approaching the copper, we measured an enormous drop in quality factor of the cantilever towards below $Q < 1000$. This is caused by the eddy currents of the copper induced by the magnetic fields of the magnetic particle attached to the cantilever. Due to this drop in quality factor, we were not able to determine the initial height above the copper with more than 0.5 μm precision.

[1]Korringa relation: A relation for metals in which $\frac{1}{T_1}$ is proportional to the temperature. The relaxation process is induced by a simultaneous flip of the free electron spins and the nuclear spins. The energy for this process is provided by the scattering of the electrons (change in kinetic energy of the electron), with energy $\hbar(\omega_e - \omega_n)$, where ω_e and ω_n are the larmor frequency of the electron spin and the nuclear spin respectively [107, p. 363][108, p. 121].

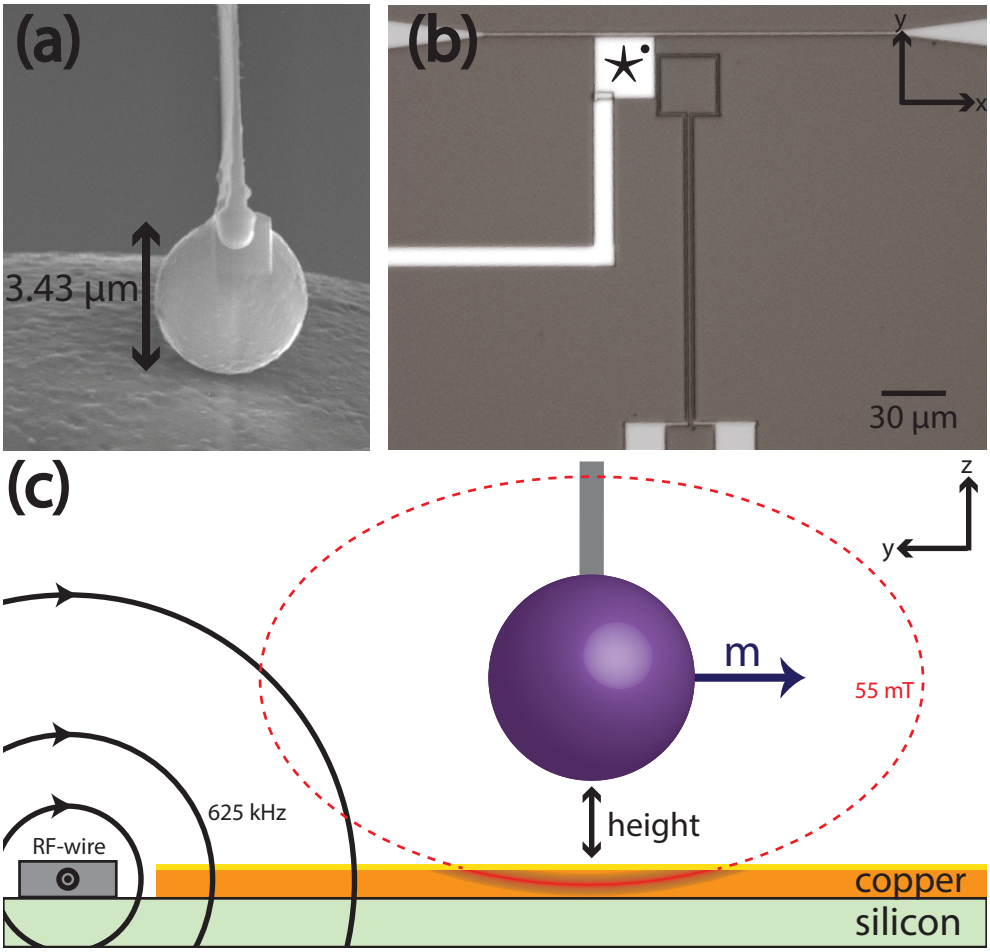

Figure 7.1: **a**) Scanning electron microscope image of the magnetic particle after it is glued to the cantilever using electron beam induced deposition from a platinum containing precursor gas. **b**) Optical microscope image of the detection chip. The horizontal wire at the top is the NbTiN RF wire. The $\star$ indicates the gold capped copper sample which is connected to a wire used for thermalization. The small black dot is where we perform the MRFM experiments presented in this chapter. Next to the sample and below the RF wire is the pick-up coil for detection of the cantilever's motion. **c**) Schematic drawing of a side view of the local NMR experiment.

Nuclei close to the magnetic particle experience a magnetic field $\boldsymbol{B}(\boldsymbol{r})$ and the gradients of the magnetic field provide a coupling with the magnetic cantilever, which results in an effective frequency shift per spin on the natural frequency f_0 of the cantilever [109, 97]. The alignment of the nuclear spins will be perturbed when a radio-frequent pulse with frequency f_{RF} is applied to the sample. We call the volume containing the spins that meet the resonance condition $hf_{RF} = \gamma B(\boldsymbol{r})$ the resonance slice. When the spins are inverted, the cantilever will experience a frequency shift $-2\Delta f_0$, while for ensembles of spins that lose their net Boltzmann polarization the

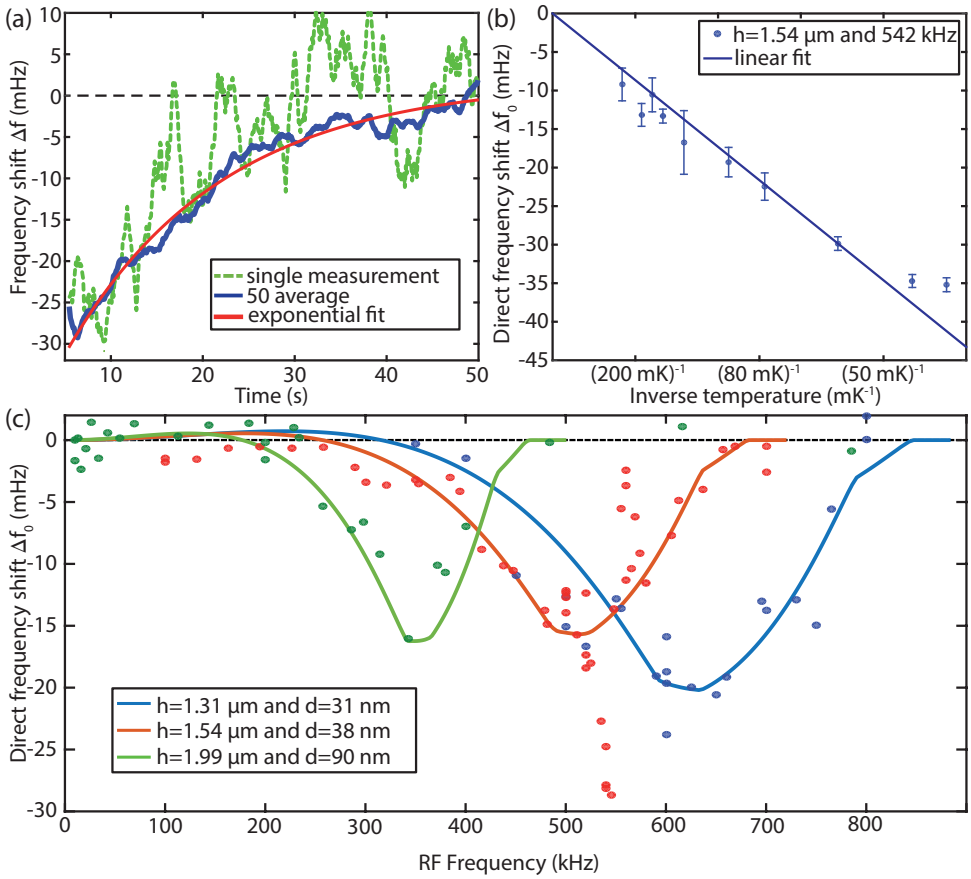

Figure 7.2: **a**) At $t = 3$s a RF-pulse with a pulse width of one second saturates all spins within a resonance slice resulting in a direct frequency shift Δf_0 of the cantilever's resonance frequency. The shift relaxes with the nuclear spin's relaxation time T_1. The dashed green line shows a single measurement of the frequency shift (with a moving average of 1 second), the solid blue line shows 50 averages. The red solid line is an exponential fit according to equation 7.1. From the fit we extract the direct shift Δf_0, extrapolated at $t = 4$ s directly after the pulse, and relaxation time T_1. **b**) The direct frequency shift Δf_0 versus temperature. The linear fit is expected according to Curie's law $M \propto T^{-1}$. **c**) Δf_0 as function of RF frequency f_{RF} for three different cantilever heights. The solid line is a simulation with the cantilever height z and resonance slice width d as the only fitting parameters.

frequency shift will be $-\Delta f_0$. The latter effect can easily be obtained at very low radio frequent magnetic fields in a saturation experiment, ensuring no heating of the sample at very low temperatures.

Taking the approximation of a circular wire, we estimate the typical field strength $B_1 = \frac{\mu_0 I}{4\pi r} \approx 2.8\mu$T, for a current of 0.2 mA. We assumed that the RF field is perpendicular to the static field B_m, even though this is not always the case (see figure 7.1c). With this, we can calculate the saturation parameter $s \equiv \gamma^2 H_1^2 T_1 T_2$. We see that for the expected relaxation times $T_1 > 5$ s and $T_2 = 0.15$ ms we obtain a saturation

parameter in the order of 1, showing that the spins will be at least 50 % saturated. Note that this only holds for spins exactly at the resonance condition, and since we work with field gradients, we always have spins that do not fully saturate. For the sake of simplicity, we assume that we have a resonance slice thickness d, within which the spins are fully saturated. Since we apply pulses of 1 second, we expect a full saturation of all levels (in pure copper, no quadruple interaction is expected) , and according to Suter et al. [110], we expect that after the pulse the magnetization will restore according to a single-exponential, with a decay time equal to the spin lattice relaxation time T_1. Since our frequency shift of the cantilever is proportional to the magnetization, we can fit our data with:

$$\Delta f(t) = f_0 + \Delta f_0 \cdot e^{-(t-t_0)/T_1} \tag{7.1}$$

We use the Phase Locked Loop (PLL) of a Zurich Instruments Lock-in amplifier to measure the shifts in resonance frequency of the cantilever at a bandwidth of 40 Hz. The measurement scheme is as follows: Between $t = 0$ s and $t = 3$ s the resonance frequency of the cantilever f_0 is measured using a PLL. At $t = 3$ s the PLL is turned off and the RF current is turned on. At $t = 4$ s the RF current is turned off. Around $t = 5$ s the PLL is turned on and measures the frequency shift relative to f_0. The reason we switch off the PLL during the RF pulse and turn it back on one second after the RF pulse, is to avoid crosstalk.

The RF current of 0.2 mA is applied using a function generator. The current is chosen in such a way that the saturation parameter is much larger than 1. For currents larger than 1 mA we observe a temperature increase at frequencies larger than 1 MHz. The dissipation of our RF wire will be subject of further study. In this report we stay away from the maximum currents at the applied frequencies before heating.

7.4 Results

In figure 7.2a, a measurement is shown at a temperature of 42 mK and a RF-frequency of 542 kHz while the cantilever was at the position used for the red curve in figure 7.2c). At the frequency of 542 kHz, the frequency shifts were larger than at other frequencies, probably due to the broadening of the resonance slice due to the excitation of a higher cantilever mode. We measured the frequency shift until $t = 50$ s. We averaged every measurement 50 times and fit it with equation 7.1. From the fit, we extracted Δf_0 and T_1. Δf_0 is plotted against temperature in figure 7.2b) and fit with a straight line according to the expected Curie's law $\Delta f_0 \propto \langle \mu \rangle \propto \frac{1}{T}$. At the lowest temperature we may see the onset of saturation of the frequency shift effect, indicating that the (electron) spins are difficult to cool, although the saturation may also have been reached because the minimum temperature of the refrigerator was reached. For every temperature we collected at least three sets of 50 curves, and the error bars are the standard deviations calculated from the three separate fits.

In figure 7.2c) the direct frequency shift is plotted versus RF frequency for three different cantilever heights. The height is controlled by changing the voltage of the

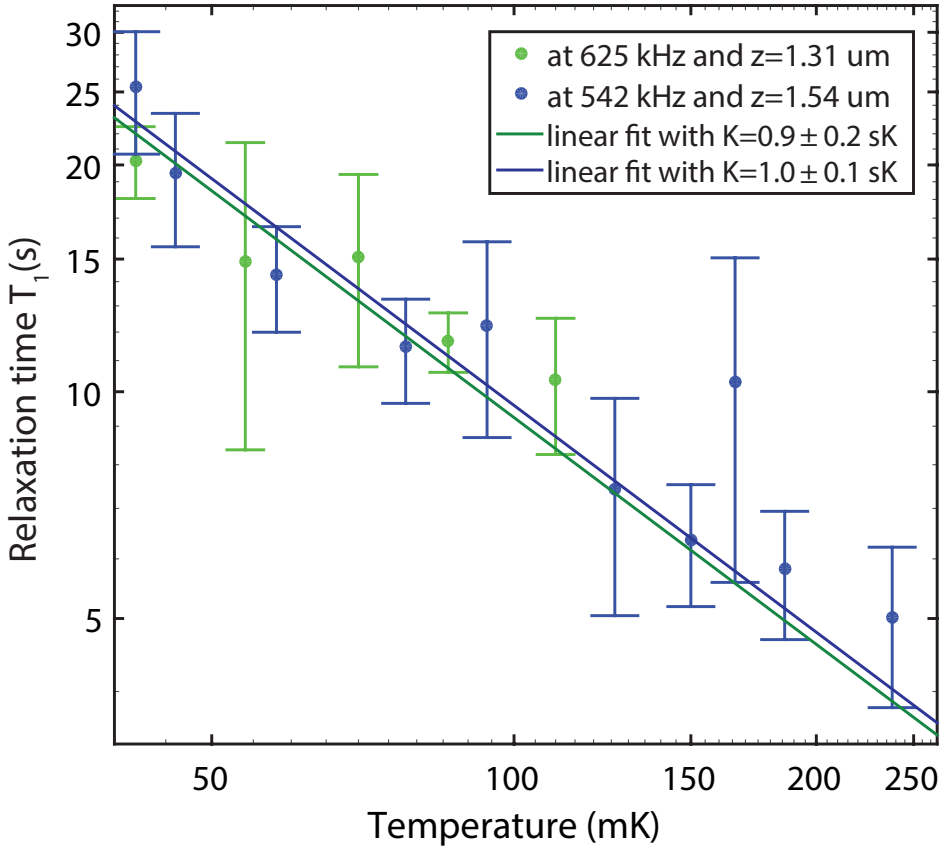

Figure 7.3: The inverse of the relaxation time of the copper nuclei measured by applying saturation pulses versus temperature. We find the same linear dependence with temperature as is found in bulk copper samples, the so called Korringa relation. In blue, the data is measured at a height of 1.54 μm at 542 kHz. In green, the data is recorded at 1.31 μm and at a frequency of 625 kHz. We find $\kappa = 1.0 \pm 0.1$ sK and $\kappa = 0.9 \pm 0.2$ sK respectively with a linear fit with the error indicating the 95 % confidence intervals. Every data point is an average of at least three sets of averaged data. The error bars give the standard deviation of the relaxation times for the averaged data sets.

finestage below the sample. Every data point resembles a dataset of 50 averaged single measurements. The solid line is a fit to the data, with the only fitting parameters the resonance slice width and height of the cantilever. The stiffness and magnetization of the cantilever is extracted from previous measurements [97]. The height of the cantilever is left as a fitting parameter, because the absolute height is not known with sufficient accuracy, since the piezo-stack in the finestage behaves nonlinear.

For two different RF frequencies, 542 kHz and 625 kHz, at two different heights of the cantilever, 1.54 μm and 1.31 μm, we measured the relaxation time T_1 as a function of temperature to verify the local temperature. The results are shown in figure 7.3. From the straight fits we extract the Korringa constant $\kappa = 1.0 \pm 0.1$ sK and $\kappa = 0.9 \pm 0.2$ sK, which is close to the expected value of the combined ^{63}Cu and

Table 7.1: NMR constants and parameters for copper [111, 112, 113, 84].

parameter	variable	Value
Radius magnet	R_0	3.43/2 μm
Magnetization	RMT	1.15 T
Copper layer thickness	d_{Cu}	300 nm
Gyromagnetic ratio ^{63}Cu	γ_{63}	11.3 MHz/T
Gyromagnetic ratio ^{65}Cu	γ_{65}	12.1 MHz/T
Natural abundance ^{63}Cu		69 %
Natural abundance ^{65}Cu		31 %
Spin-Spin relaxation time	T_2	0.15 ms
Korringa constant ^{63}Cu	κ_{63}	1.27 sK
Korringa constant ^{65}Cu	κ_{65}	1.09 sK
Local field	B_{loc}	0.34 mT

^{65}Cu Korringa constants which is $\kappa = 1.2$ sK [84, p. 225].

In the simulations (solid lines in Figure 2c), we have employed the formula's for the frequency shifts as they were calculated by De Voogd et al. in reference [109] with the parameters for copper (Table 7.1). Several things contribute to the width of the resonance slice, as will be described below. This leads to the resonant slice thickness not being the same everywhere in the slice. For the simulations of this experiment we have taken the resonant slice thickness to be uniform over the resonant slice.

7.5 Discussion

7.5.1 The Korringa constant

Let us first discuss the comparison between the Korringa constants we found, $\kappa = 1.0 \pm 0.1$ sK and $\kappa = 0.9 \pm 0.2$ sK, and the expected value based on the natural abundances and Korringa constants of the two copper isotopes (Table 7.1) of $\kappa = 1.2$ sK for bulk NMR measurements. We see a possible small deviation, which we may or may not attribute to the different mechanisms enumerated below.

First, there is the effect of flip-flop processes between nuclear spins which gives diffusion of the saturated magnetization. if the diffusion after several seconds is larger than the typical length scales at which the coupling with the cantilever decays, this can be a considerable effect. To explore this possibility, we first need to calculate the spin diffusion constant.

For poly-crystalline copper, we find a transition rate of $W = \frac{1}{30T_2}$ [107, p. 138-139] [114]. We use $T_2 = 0.15$ ms and we find $W = 2.2 \cdot 10^2$ s^{-1}. Our field gradients are too small to suppress the spin diffusion [115]. The nearest neighbor distance a is 0.256 nm [116, p. 24]. This gives us a spin diffusion constant of $D = Wa^2 = 15$ nm^{2}s^{-1}. This yields a diffusion length, l_D, after one second of $l_D = 2\sqrt{Dt} = 7.6$ nm. For the lowest temperature of 42 mK, we expected a Korringa constant of 28 seconds, resulting in $l_D = 40$ nm. We measured the Korringa relation at a position where a maximum signal was obtained. The signal when the spin has moved 40 nm further

in the x-direction can be calculated to have an estimate if this can have affected the observed Korringa relation. We see for the frequency of 625 kHz a reduction of the magnetization of approximately 10%. From this we can say that the lower Korringa relation could possibly be caused by the spin diffusion of the saturated magnetization in the resonance slice towards areas where the coupling with the cantilever is smaller. Also, the spin diffusion can possibly give an additional relaxation channel [107, p. 139].

A second mechanism to obtain a shorter T_1 time is discussed by [112] and may be caused by electronic magnetic impurities. Also in reference [111] it is discussed that tiny impurities can alter the Korringa constant. We don't expect impurities to play a big role, because the copper was capped with gold. However, the dangling bonds at the surface of the silicon substrate [97] could have been an additional relaxation channel for nearby copper nuclei.

7.5.2 The resonance slice thickness

We also would like to discuss the resonant slice thickness we found, since this is important for the resolution of possible future imaging or spectroscopic experiments, or when similar measurements are performed on much thinner films.

First, there is the width of the Lorentzian resonance curve in a conventional magnetic resonance experiment [107]. The full width half maximum (FWHM) is equal to twice the Rabi frequency. In our case that is approximately 6 μT. When this number is divided by the field gradient $|\nabla_r \boldsymbol{B}(\boldsymbol{r})|$ which is up to $5 \cdot 10^4$ T/m, we obtain a thickness $d = 0.1$ nm, which cannot account for the found resonance slice thickness by the simulation in figure 7.2c).

Secondly, we need to consider the motion of the cantilever itself. We estimate from the quality factor at each height and the piezo's drive amplitude, that we drove the cantilever 60, 37 and 100 nm respectively for the found slice thicknesses of 90, 38 and 31 nm. The cantilever's motion is in the x-direction, while in our simulation, we take in the resonance slice thickness in the radial direction. When we perform the simulation and take the slice thickness only in the x-direction, we see a best fit with the data for a cantilever motion of approximately 250, 100 and 90 nm respectively. From this we conclude that a resonance slice thickness only determined by the motion in the x-direction of the cantilever is not likely, and that there is another mechanism that broadens the resonance slice in the radial direction.

One possibility to broaden in the radial direction is the effect of the local fields. The copper nuclei have an internal field of 0.34 mT, caused by direct coupling with neighbors and by indirect coupling via conduction electrons with neighbors. We can approximate the internal field as a Gaussian distribution. During a RF pulse, the spin can feel a different local magnetic field due to a changing environment, or the spin can flip-flop with a neighboring spin [114]. The flip-flop speed is $W = 2.2 \cdot 10^2$ s^{-1}, as calculated before, and the number of Rabi oscillations with the one second pulse is $\gamma B_1 \cdot 1$ s $\approx 3 \cdot 10^1$. From these numbers we can conclude that it is likely that the resonance slice is broadened by approximately the distribution of the local magnetic field. When we take the obtained resonance slice thicknesses of 90, 38 and 31 nm, we calculate that we need a broadening of 6.3, 4.3 and 4.6 times the average local field strength respectively. These numbers are not unlikely, considering that within

a small volume only a small fraction of spins needs to have the exact local field to meet the resonance condition within $|\boldsymbol{B}(\boldsymbol{r}) - \boldsymbol{B_1}| < |\boldsymbol{B}(\boldsymbol{r}) + \boldsymbol{B_{loc}}| < |\boldsymbol{B}(\boldsymbol{r}) + \boldsymbol{B_1}|$, after which the flip-flops or the changing environment can destroy the magnetization of the whole ensemble.

7.6 Conclusion

To summarize, we have performed nuclear magnetic resonance force microscopy experiments down to 42 mK. We verified the local temperature by verifying the Korringa relation for copper. Since this relation is a direct probe of the electronic susceptibility of the material, we believe that MRFM may prove to be a useful tool for measuring novel quantum materials.

-